Effects of Large-Scale Wind Driven Turbulence on Sound Propagation

John M. Noble
U.S. Army Atmospheric Sciences Laboratory
ATTN: SLCAS-AS-I
White Sands Missile Range, NM 88002

Henry Bass and Richard Raspet
Physical Acoustics Research Group
Department of Physics and Astronomy
The University of Mississippi
University, MS 38677

Abstract

Acoustic measurements made in the atmosphere have shown significant fluctuations in amplitude and phase resulting from the interaction with time varying meteorological conditions. The observed variations appear to have short term and long term (1-5 minutes) variations at least in the phase of the acoustic signal. One possible way to account for this long term variation is the use of a large scale wind driven turbulence model. From a Fourier analysis of the phase variations, the outer scales for the large scale turbulence is 200 meters and greater, which corresponds to turbulence in the energy-containing subrange. The large scale turbulence is assumed to be elongated longitudinal vortex pairs roughly aligned with the mean wind. Due to the size of the vortex pair compared to the scale of our experiment, the effect of the vortex pair on the acoustic field can be modeled as the sound speed of the atmosphere varying with time. The model provides results with the same trends and variations in phase observed experimentally.

Effects of Large Scale Wind Driven Turbulence on Sound Propagation

Introduction

Random fluctuations in the acoustical index of refraction in the atmosphere is the result of the presence of turbulence. These random fluctuations in the acoustical index of refraction results in fluctuations of the amplitude and phase of an acoustic wave. The variations in the amplitude and phase show changes occurring over two different time scales. The short term variations correspond to turbule sizes on the order of 1 meter, while the long term variations seem to correspond to turbule sizes on the order of 100 m and greater.

The aim of this work was to develop a descriptive model for large scale wind driven turbulence and the effects of large scale turbulence on the sound field. The model will describe the shape and horizontal and vertical wind velocity profiles for the turbulence. Due to the size of the turbules in relation to the experiment conducted, a simple phase model was developed to perform phase variation calculations using the results from the large scale turbulence model.

Atmospheric Effects

Before the model for the large scale wind-driven turbulence is presented, lets first examine the dynamics of the atmosphere. In discussing the details of air flow, it is convenient to consider the atmosphere to be divided into a number of horizontal layers (figure 1). The region in which the atmosphere experiences surface effects through vertical exchanges of momentum, heat, and moisture is called the planetary boundary layer (PBL) or is sometimes referred to as the friction layer. Panofsky and Dutton[1] defines the depth of the PBL, h, as the thickness of the turbulent region next to the ground which is also called the mixing layer. Another height used to describe the thickness of the PBL in the daytime is the height z_i of the lowest inversion. Actually, h tends to be roughly 10% larger than z_i because the lowest part of the inversion is still turbulent, partly because of overshooting from below, partly because there is often strong wind shear in the inversion.

The lowest part of the PBL is called the surface layer. In this layer, the characteristics of turbulence and the vertical distribution of mean variables are relatively simple. There is no precise definition of the surface layer. Qualitatively, the surface variations of vertical fluxes can be ignored. Typically, the fluxes are large at the surface and decrease to zero near the top of the PBL.

The main problem is calculating the height of the lowest inversion z_i. This value is important since it represents the largest size an inhomogeneity can be in the atmosphere. According to Panofsky and Dutton[1], the horizontal wind speed fluctuations are related to z_i by

$$\frac{\sigma_u}{u_*} = (12 - 0.5\frac{z_i}{L_{mo}})^{1/3} \tag{1}$$

where u_* is the friction velocity and L_{mo} is the Monin-Obukhov length. If variations in the horizontal wind speed are due to purely mechanical turbulence, an alternate formula for u_* can be used for $z > z_o$:

$$u_* = \frac{uk}{ln(z/z_o)} \tag{2}$$

where k is the von Karmon constant (0.4), u is the horizontal wind speed at height z, and z_o is the roughness length. Substituting equation (2) into equation (1) and solving for z_i results in

$$z_i = 2L_{mo}[12 - (\frac{\sigma_u}{ku})^3 ln^3(z/z_o)] \tag{3}$$

This provides the height of the lowest inversion in terms of Monin-Obukhov length, the fluctuation of the horizontal wind speed, and the roughness length. The Monin-Obukhov length can be estimated using tables 1 and 2 knowing the surface wind, incoming solar radiation, and the roughness length (for table 2, the roughness length was 0.05 meters for the experiments[1]).

Experimental Procedure and Data Analysis

A series of line-of-sight propagation measurements were made over relatively flat open farm land. A run consisted of an eight minute record of signals received simultaneously at five transverse microphones mounted one meter above the ground and one microphone mounted near the source for a reference (figure 2). The sound source was driven by a tape with a prerecorded signal consisting of a mixture of eight tones centered at one octave spacings beginning at 62.5 Hz. This geometry is similar to the geometry Daigle[2,3] used in his experiments.

The meteorological data was collected using a series of three-cup anemometers and temperature probes at four heights; 3, 10, 30, and 110 ft. The data acquisition system provided a five minute period of wind speed, wind direction, and temperature as well as the maximum and minimum values during the five minute period. Measurements of the fluctuating wind speed and temperature data were also made using the techniques outlined by Johnson[4].

The Fourier transform of the amplitude and phase variations contains the spectrum of the fluctuations of the sound field due to turbules present

in the atmosphere. The spectral peaks are related to the scale of turbulence L by "Taylor's hypothesis of frozen turbulence" which relates the temporal and spatial turbulence scales by[5]

$$L = \overline{u}\tau \tag{4}$$

where $\overline{u}$ is the mean wind speed and τ is the characteristic time associated with the temporal measurements. Taylor's equation can be rewritten as

$$L = \frac{\overline{u}}{\nu} \tag{5}$$

where $\nu = 1/\tau$. Calculations of L show the different scales of turbulence present in the atmosphere during the experiment. Figure 3 is for a run where the wind speed is low. The spectrum shows several peaks which represent the different scales of turbulence present in the atmosphere for that run. Figure 4 is for a run where the wind speed is high. The only spectral peak present is one at a low frequency. This implies that the only scale of turbulence which is affecting the phase is on the order of a few hundred meters in size.

Some caution must be noted here about this type of analysis. The location of the low frequency peak may be a result of insufficient frequency resolution due to the length of the sample analyzed. A longer time sample might shift the low frequency peak to even lower frequencies.

The Fourier transform for the amplitude variations were also computed. There is not a spectral peak for the amplitude at the low frequency end of the spectrum. Large scale variations in the atmosphere cause changes in the sound field resulting in refractive variations instead of a scattering process as in small scale turbulence.

Large Scale Turbulence Model

The first problem is to obtain, from experimental measurements, a clear idea of the structure and motion of the turbulence. From now on, frequent references will be made to 'eddies' of the turbulent motion, a word intended to describe flow patterns with spatially limited distributions of vorticity and comparatively simple forms. Since the experimental data consists of point measurements, the identification of eddy types must be by informed guesswork followed by measurements designed to confirm the guess.

According to Tennekes,[6] there appears to exist in all turbulent shear flows more or less distinct large eddies with relatively long lifetimes. Townsend was the first to investigate the structure and dynamics of these large scale vortices.[7] Townsend was struck by the fact that in all turbulent shear flows he knew, the eddy viscosity K_m, nondimensionalized by appropriate length and velocity scales, turned out to be a number that is relatively independent of the flow considered. Townsend hypothesized that the large eddies must be responsible for this universality. According to

Townsend, the eddies are elongated longitudinal vortex pairs in the boundary layer, roughly aligned with the mean flow, figure 5.

The lifetimes of the eddies are greater than the length of time for data runs discussed here. For this analysis, they will be considered to be "permanent". Note that secondary circulations cause local regions of horizontal convergence near the surface. Those regions are the sites of vigorous turbulence production rates, and may be responsible for the generation of most of the Reynold stress in the boundary layers. Tennekes concludes that the eddies are capable of relatively long lifetimes because the mean shear is an adequate source of energy.

If a stream function $f(x,z)$ for a particular arrangement of eddies is known, there are several parameters of the eddy system which can be calculated. Stream functions are a type of function which describe the streamlines in a flow. Streamlines are regions where the velocity vectors of the fluid are tangent at a particular instant. The velocity distribution of the eddy can be calculated using[8]

$$u(x,z) = -\frac{\partial f(x,z)}{\partial z} \tag{6}$$

and

$$v(x,z) = \frac{\partial f(x,z)}{\partial x} \tag{7}$$

where $u(x,z)$ and $v(x,z)$ are the horizontal and vertical wind speeds respectively. The functional form of the stream function which represents an eddy pair is[7]

$$f(x,z) = A[cos(lx) + e^{-l^2/\alpha_x^2}]e^{-\frac{1}{4}\alpha^2 r^2} \tag{8}$$

where A is a constant specifying the intensity of the eddy pair, $\alpha^2 r^2 = \alpha_x^2 x^2 + \alpha_z^2 z^2$, l is the characteristic wavenumber of the eddy pair, and α_x and α_z are the horizontal and vertical wavenumbers for the eddy pair. The coordinates (x,z) are relative to the center of the eddy pair. Townsend uses a characteristic wavenumber for the eddy pair of $\pi\alpha_x$.

Using equations (6) and (7), the horizontal and vertical wind speed are

$$u(x,z) = B\alpha_z^2 z[cos(lx) + e^{-l^2/\alpha_x^2}]e^{-\frac{1}{4}\alpha^2 r^2} \tag{9}$$

and

$$v(x,z) = -B\{2lsin(lx) + \alpha_x^2 x[cos(lx) + e^{-l^2/\alpha_x^2}]\}e^{-\frac{1}{4}\alpha^2 r^2} \tag{10}$$

where $B = A/2$. Figure 6 is the horizontal wind speed versus height for x = 0 m, $\alpha_x = 0.0043\ m^{-1}$, $\alpha_z = 0.0087\ m^{-1}$, and $B = 2000\ m^2/s$. The negative height refers to a vertical position below the center of the eddy pair. Figure 7 is the horizontal wind speed versus range for z = -150 m using the same parameters as in the previous figure. The negative range refers to a horizontal position to the left of the center of the eddy pair.

For this work, the size and intensity of the eddy pairs were determined from meteorological data taken in the field. The standard deviation of the wind speed was calculated using a TSI hot wire anemometer. Using the standard deviation of the wind speed, the roughness length, the wind speed at height z, and estimating the Monin-Obukhov length from table 2, the height of the lowest inversion layer z_i is calculated using equation (3). This provides a maximum height of the eddy pair. The Fourier transform of the phase variation provides an estimate of the lower limit for the horizontal extent of the eddy pair. For the data analyzed, the average of the wind speed over five minutes at a given height remains essentially constant for successive five minute periods; the maximum and minimum variations in the wind speed must occur within that five minute period. Assuming that the eddy pair is carried by the mean wind, the maximum horizontal length scale is just the mean wind times five minutes.

The information known at this point allows α_x and α_z to be estimated. Next, the variational constant B of the eddy pair must be estimated. The value of B in equation (9) is varied until the fluctuation of the horizontal wind speed agrees with the maximum and minimum wind speeds recorded over a five minute period on the tower. With these three parameters estimated, the eddy pair model will provide the horizontal and vertical wind speed with range and height.

Determination of Eddy Pair Parameters

The meteorological data consisted of five minute averages with the maximum and minimum of the wind speed in that period. A direct calculation of the scale sizes of the eddy pairs can not be made since they typically passed the tower in less than five minutes. The procedure used to determine the eddy pair parameters outlined in the previous section is used for the experimental runs examined.

The first experiment to be examined is Run 2.1 of January 11, 1985. The important constants are the mean wind speed, the horizontal and vertical wavenumbers, and the constant, B, for the eddy pair. The mean wind speed is calculated from the meteorological profiles of the experimental runs by performing a curve fit to equation (2). The procedure to determine the horizontal and vertical wavenumbers is to use equation (3) for calculating the height of the first inversion layer and using this height to calculate the vertical height of the eddy pair. The curve fit to equation (2) provides values for the roughness length and the friction velocity. The horizontal wind speed fluctuation, σ_u, is determined from the hot wire measurements. Using the mean wind speed and incoming solar radiation, the Monin-Obukhov length can be estimated from table 2.

For the experiment in question, the day was overcast with a light wind of 3.3 m/s. Using tables 1 and 2 for incoming solar radiation and a surface wind speed of 3.3 m/s, the Monin-Obukhov length, L_{mo}, was estimated to be 20 meters. From analysis of the five minute wind speed measurements

with height, the horizontal wind speed fluctuation was 0.40 m/s. For the experiments discussed, the roughness length was estimated from table 3 to be 0.05 meters. Using these parameters, the height of the first inversion layer was calculated to be 450 meters using equation (3).

Using the condition that the eddy pair traverses past the tower within a five minute period, the maximum eddy pair size possible to traverse the field of propagation is 990 meters. If the dimensions of each eddy are 450 m, then the eddy pair has a horizontal length of 900 meters. This size is less than the maximum size constraint dictated by the five minute measurement period. Using equation (9), the horizontal and vertical wavenumbers (α_x and α_z) for the eddy pair are 0.125 m^{-1} and 0.025 m^{-1}.

To determine the constant B in equation (9), the maximum and minimum wind speed fluctuations within a five minute segment with height are compared with the wind speed fluctuations predicted by the model. The parameter B is varied until the predicted wind speed variations fit those observed for a five minute segment. For the date in question, the value of B which best fit the data is 200 m^2/s.

The next experimental run was Run 1.1 of December 13, 1984. This day differed from January in that the mean wind speed and horizontal wind speed fluctuations were much greater. The mean wind speed was 6.3 m/s while the horizontal wind speed fluctuation was 1.0 m/s. Table 6.6 in Panofsky and Dutton[1] is used to determine the value of L_{mo}. Using this table, the value of L_{mo} is estimated to be on the order of 100 to 150 m, which gives a value for z_i of 575 to 875 m.

Results From the Eddy Pair Model

Viewing the movement of the eddy pair on the scale of the geometry of the experiments, the variation of the sound speed in the atmosphere would appear to change slowly over the entire range of the experiment uniformly. Using a simple model of the wind speed in the atmosphere slowly varying from u_1 to u_2, the expected phase change can be calculated using

$$\Delta\varphi = \frac{2\pi f R}{c_o^2}(u_1 - u_2) \tag{11}$$

where R is the propagation distance, c_o is the sound speed at temperature T, and f is the frequency of the signal. A comparison between the magnitude of the phase change for the simple model and the experimental results is shown in table 3.

Conclusions

Experimental acoustic phase data definitely displays two variational time scales. The short term time variations can be attributed to the presence of small scale turbulence present in the atmosphere. The small scale turbulence does not account for the longer time variations in phase.

The large scale turbulence model is composed of pairs of vortices or eddies moving through the atmosphere at the mean wind speed. The scale parameters for the eddy pairs are determined from the available meteorological data composed of the maximum, minimum, and average wind speed over a five minute segment for four heights and meteorological theories of the behavior of the lower atmosphere. The constraint of the eddy pair moving through the field of propagation within five minutes is generally used as an upper bound for the dimensions of the eddy pair; however, it could be used as the size of the eddy pair if there is lack of available meteorological data.

The results of the eddy pair model were used to examine the phase fluctuations of the acoustic wave using a simple phase model. The input parameters for the model were determined from analysis of the acoustical and meteorological data collected in the experiments. The magnitude of the phase variations predicted using this model was found to be in very good agreement with the experimental results.

References

1. H.A. Panofsky and J.A. Dutton, *Atmospheric Turbulence: Models and Methods for Engineering Applications*, (Wiley, New York, 1984).

2. G.A. Daigle, J.E. Piercy, and T.F.W. Embleton, "Line-of-Sight Propagation Through Atmospheric Turbulence Near the Ground," J. Acoust. Soc. Am. **74**, 1505-1513(1983).

3. G.A. Daigle, T.F.W. Embleton, and J.E. Piercy, "Propagation of Sound in the Presence of Gradients and Turbulence Near the Ground," J. Acoust. Soc. Am. **79**, 613-627(1986).

4. M.A. Johnson, R. Raspet, and M.T. Bobak, "A Turbulence Model for Sound Propagation from an Elevated Source Above Level Ground," J. Acoust. Soc. Am. **81**, 638-646(1987).

5. G.A. Daigle, J.E. Piercy, and T.F.W. Embleton, "Effects of Atmospheric Turbulence on the Interface of Sound Waves Near a Hard Boundary ," J. Acoust. Soc. Am. **64**, 622-630(1978).

6. H. Tennekes, "Similarity Laws and Scale Relations in Planetary Boundary Layers," in *Workshop on Micrometeorology*, edited by Duane A. Haugen (American Meteorological Society, Boston, 1973), pp. 177-216.

7. A.A. Townsend, *The Structure of Turbulent Shear Flow* (Cambridge University Press, New York, 1976).

8. D.E. Rutherford, *Fluid Dynamics* (Interscience Publishers Inc, New York, 1966).

Table 1. Estimation of Turner Classes.

Surface Wind Speed (at 10m), m/s	Incoming Solar Radiation		
	Strong	Moderate	Light
<2	1	1	2
2-3	1-2	2	3
3-5	2	2-3	3
5-6	3	3-4	4
6<	3	4	4

Table 2. Estimation of L_{mo} for Various Turner Classes.

Turner Class	- Lmo
1	8-12 m
2	12-20 m
3	20-60 m
4	>60 m

Table 3. Results from the Simple Phase Model for Run 2.1 of January.

Frequency (Hz)	$\Delta\varphi_{mea}(deg)$	$\Delta\varphi_{pred}(deg)$
62.5	40°	41°
125.	72°	82°
250.	155°	163°

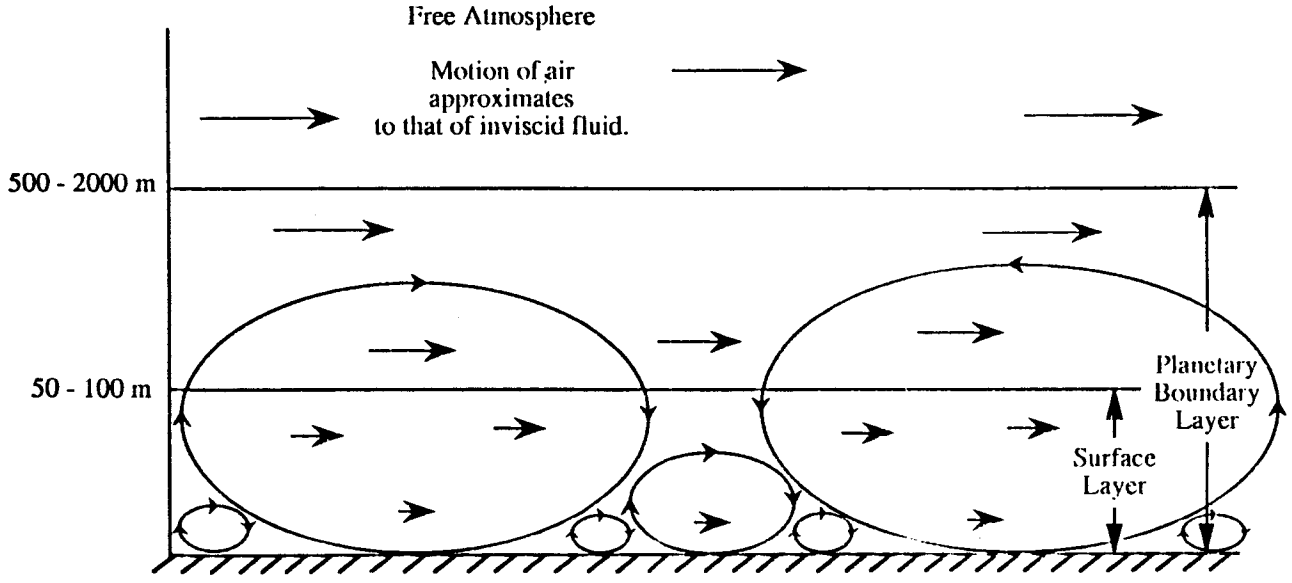

Figure 1. Breakdown of The Lower Atmosphere.

BONDVILLE, ILL.
JAN. 11, 1985
RUN 2.1

GEOMETRY

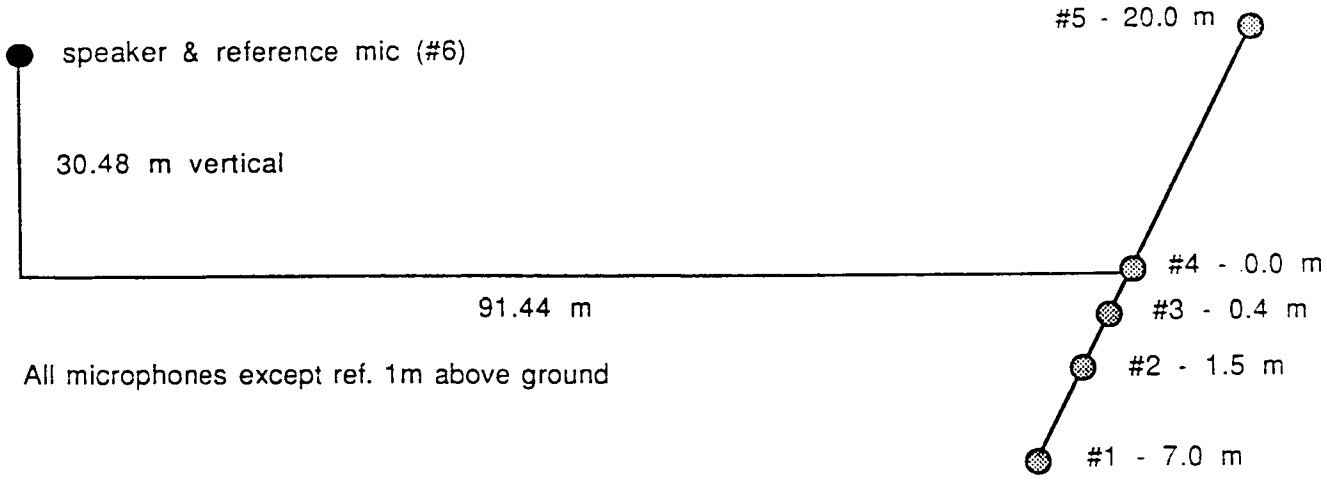

Transverse Distances		
1/2	-	5.5 m
1/3	-	6.6
1/4	-	7.0
1/5	-	27.0
2/3	-	1.1
2/4	-	1.5
2/5	-	21.5
3/4	-	0.4
3/5	-	20.4
4/5	-	20.0

Ch. #	Mic. #
1	2
2	3
3	4
4	7
5	5
6	ref
7	voice

Figure 2. Geometry For Jan. 11, 1985.

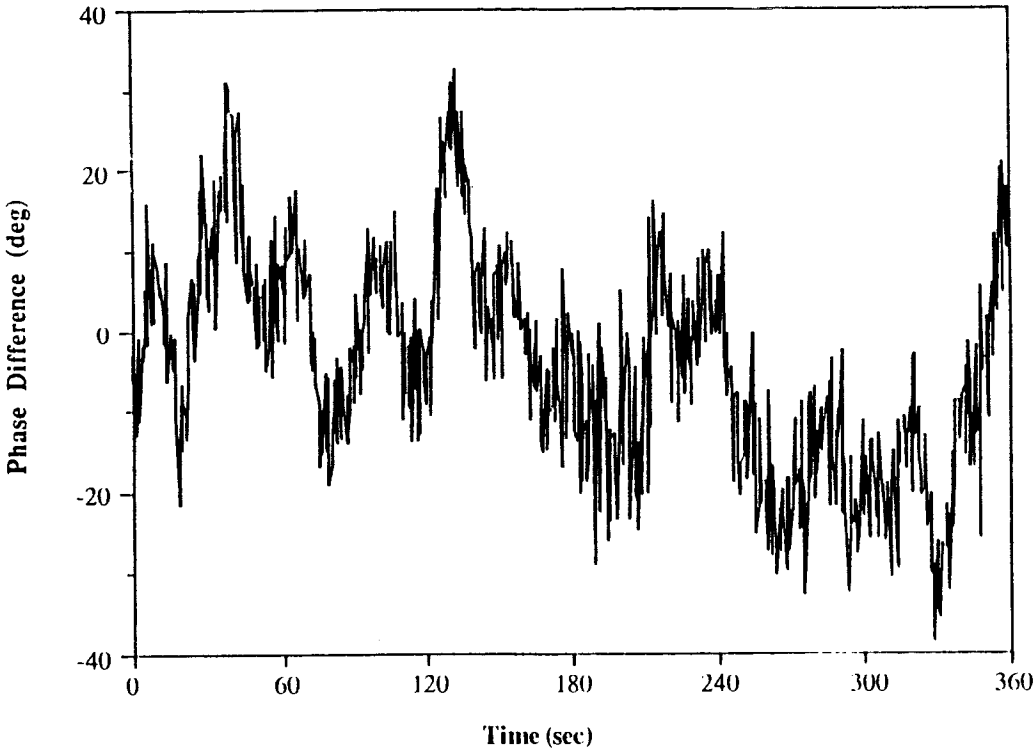

Figure 3a. Time Fluctuations for Low Wind Speed.

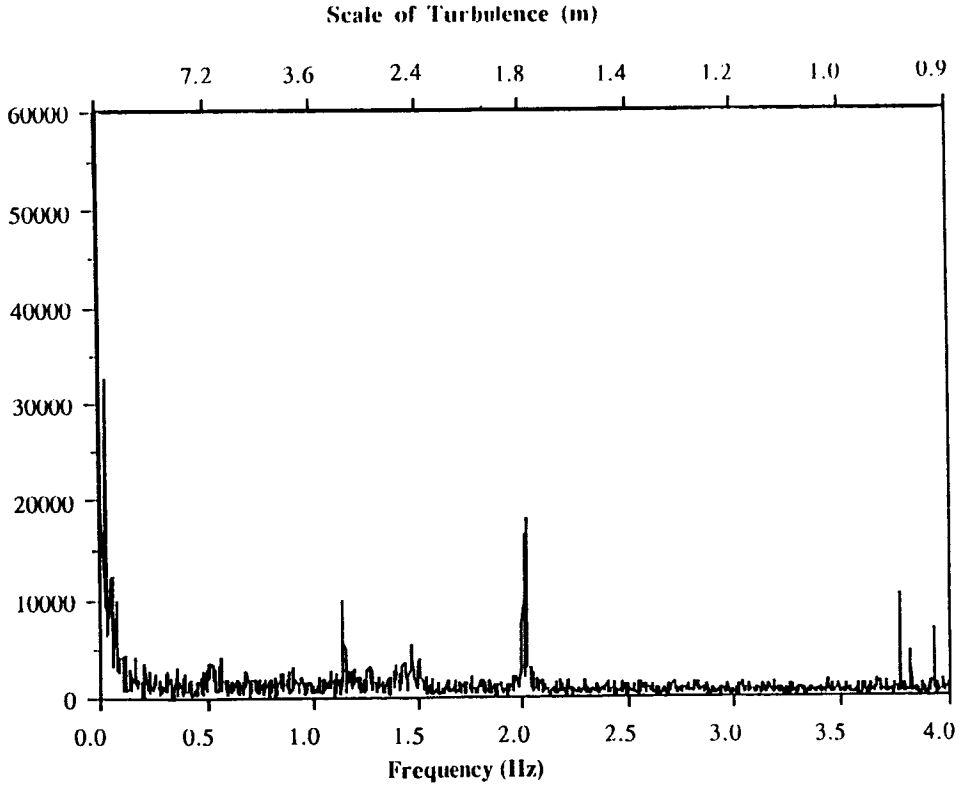

Figure 3b. Spectrum of Phase Fluctuations for Low Wind Speed.

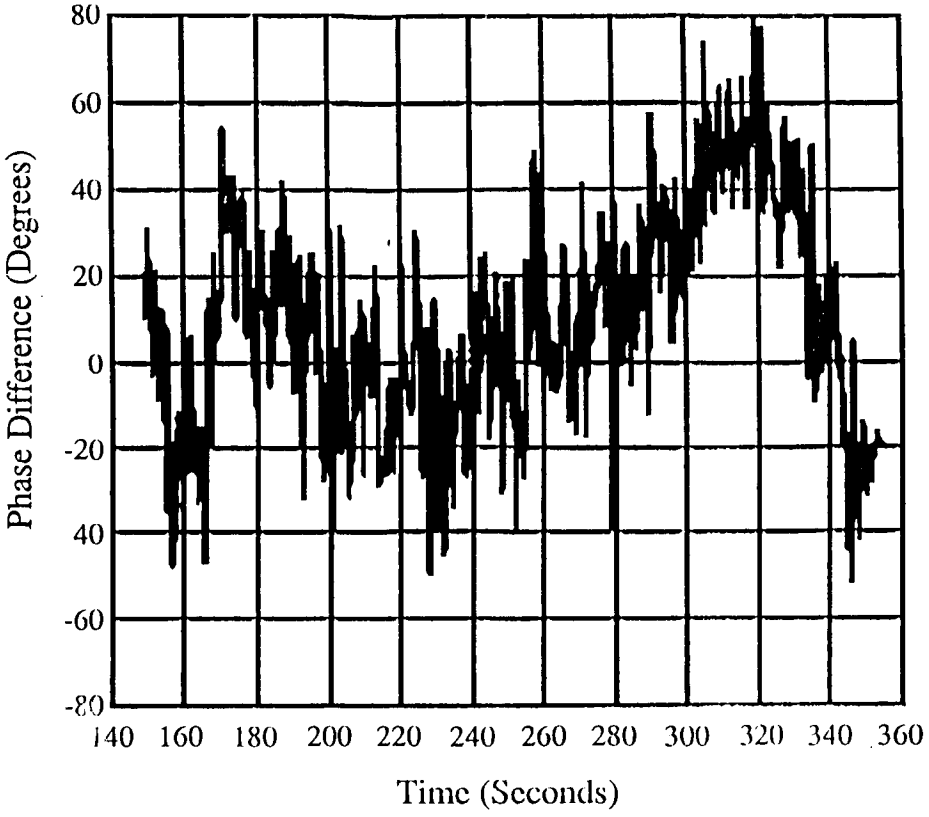

Figure 4a. Time Fluctuations for High Wind Speed.

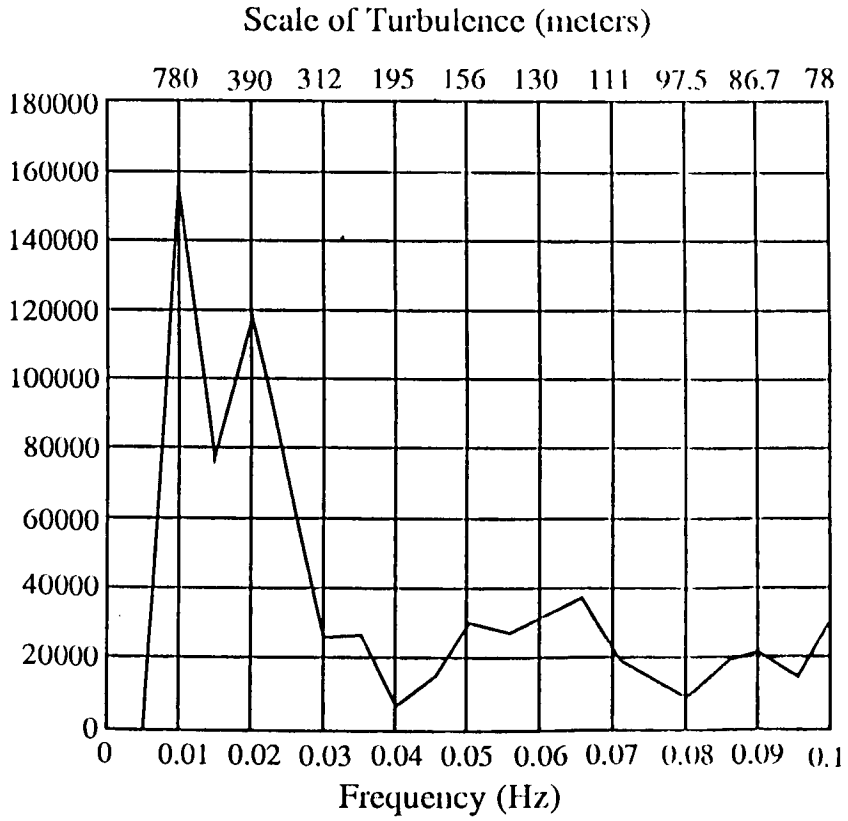

Figure 4b. Spectrum of Phase Fluctuations for High Wind Speed.

C-4

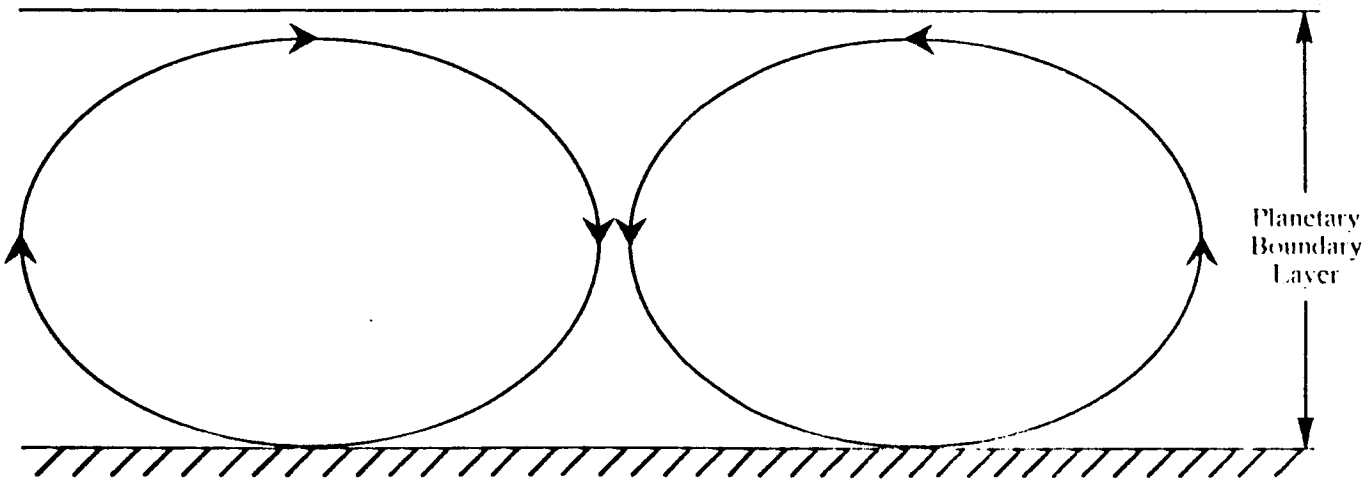

Figure 5. Illustration of Eddy Pair in the Planetary Boundary Layer.

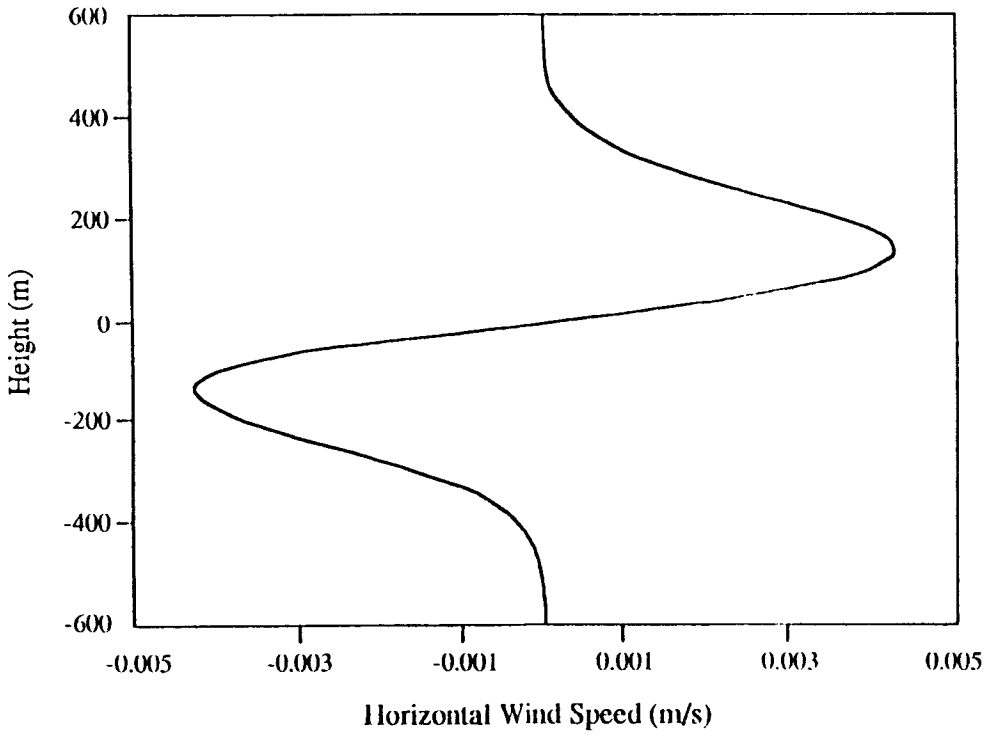

Figure 6. Horizontal Wind Speed vs. Height for $x = 0, \alpha_x = 0.0043\text{m}^{-1}$, $\alpha_z = 0.0087\text{m}^{-1}$, and $B = 2000\text{m}^2/s$.

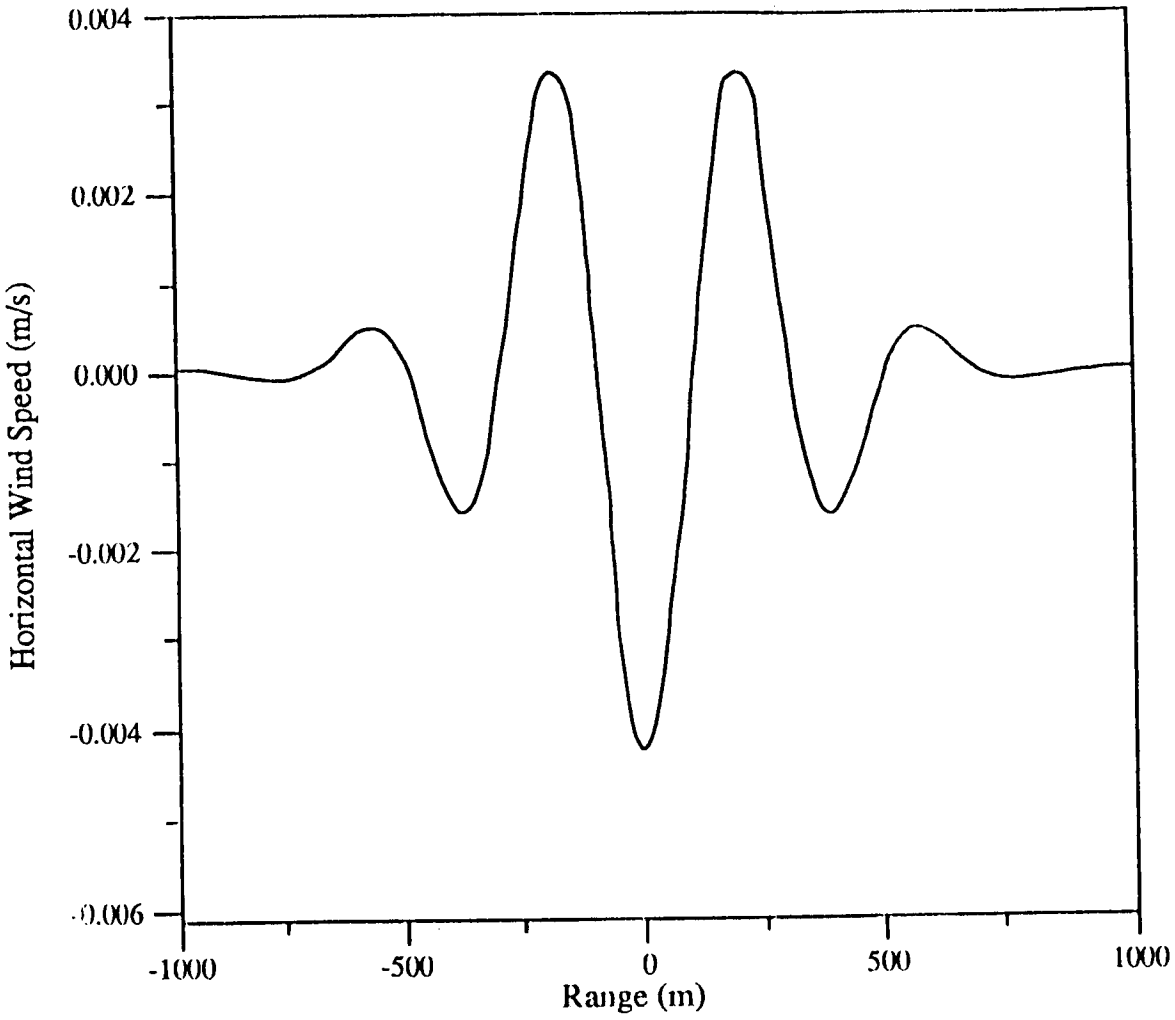

Figure 7. Horizontal Wind Speed vs. Range for $z = -150, \alpha_x = 0.0043\text{m}^{-1}$, $\alpha_z = 0.0087\text{m}^{-1}$, and $B = 2000\text{m}^2/s$.